Ab initio investigation of the pressure dependences of phonon and dielectric properties for III–V semiconductors

2005 J. Phys.: Condens. Matter 17 4475

(http://iopscience.iop.org/0953-8984/17/28/007)

INSTITUTE OF PHYSICS PUBLISHING JOURNAL OF PHYSICS: CONDENSED MATTER

J. Phys.: Condens. Matter **17** (2005) 4475–4488 doi:10.1088/0953-8984/17/28/007

Ab initio investigation of the pressure dependences of phonon and dielectric properties for III–V semiconductors

S Q Wang and H Q Ye

Shenyang National Laboratory for Materials Science, Institute of Metal Research, Chinese Academy of Sciences, 72 Wenhua Road, Shenyang 110016, People's Republic of China

E-mail: sqwang@imr.ac.cn

Received 15 April 2005
Published 1 July 2005
Online at stacks.iop.org/JPhysCM/17/4475

Abstract

Theoretical results of a first-principles plane-wave pseudopotential study on the phonon and dielectric properties for the nitrides, phosphides, and arsenides of Al, Ga, and In under hydrostatic pressure are presented. The pressure dependences of the dielectric constant, phonon frequencies at the Γ point, polarity, and localized and non-localized effective charges are calculated. We found that the dielectric constant, dynamic effective charge, and polarity decrease, while the localized effective charge and optical phonon frequencies increase with pressure for all these III–V phases. The distinctive behaviours as regards lattice dynamics of these compounds are explained on the basis of the non-localized to localized charge transference inside the crystal under pressure.

1. Introduction

Traditionally, the first-principles density-functional theory (DFT) is a method for making theoretical studies at the temperature of absolute zero. The development of density-functional perturbation theory (DFPT) allows the calculation of the phonon energies for arbitrary wavevectors from a perturbation of the primitive unit cell and therefore enables *ab initio* studies on the lattice dynamics of materials [1]. The lattice dynamics behaviour determines the thermodynamic properties of a system. First-principles investigations of many thermodynamic phenomena, such as Raman and neutron diffraction spectra, thermal expansion, specific heats, and heat conduction, have thus become feasible with the help of DFPT. First-principles computation is not only an economic way of studying materials, but also enables one to investigate the origin of a material.

The phonon dispersion is one of the main concerns for semiconductor studies. Its knowledge is essential for understanding optoelectronic behaviour, phonon–electron interactions, and carrier transportation behaviour in material. Kunc and Martin studied the dynamic properties of GaAs by means of first-principles calculations [2]. The phonon dispersions of the elemental semiconductors Si and Ge, and the III–V compounds GaAs, AlAs, GaSb, and AlSb were calculated by Giannozzi *et al* [3]. Wei and Chou reported the *ab initio* force constants and full phonon dispersions of silicon [4]. Theoretical phonon dispersions of ternary $Ga_xAl_{1-x}As$ alloys have also been calculated [5].

Understanding the effect of pressure on the phonon dispersion is quite important for many fundamental and applications studies of materials. Its knowledge allows one to correlate macroscopic thermodynamic parameters with properties on the atomic scale. Experimentally, the phonon dispersion can be determined by many modern detection techniques: neutron scattering, electron energy loss spectroscopy, IR absorption, Raman spectroscopy, etc. The diamond anvil cell has proved very convenient for direct experimental studies of many structural and physical properties of materials up to very high hydrostatic pressure. Edwards and Drickamer studied the effect of pressure on the absorption edges of some III–V, II–VI, and I–VII compounds [6]. Weinstein and Piermarini measured the Raman scattering and phonon dispersion in Si and GaP at very high pressure [7]. Trommer *et al* studied the dependence of the phonon spectrum of InP up to the pressure of the phase transition [8]. Sanjurjo *et al* explored the volume dependence of phonon frequencies for some III–V semiconductors [9]. Klotz *et al* measured the pressure induced frequency shifts of Ge up to 9.7 GPa [10]. Goni *et al* measured the effect of pressure on optical phonon modes and the transverse effective charge in GaN and AlN in Raman scattering experiments [11]. Perlin *et al* studied the pressure dependence of the transverse effective charge in wurtzite GaN single crystals [12]. In contrast with the extensive range of experimental studies on the pressure effect on the phonon dispersion of semiconductors, theoretical works on the topic are relatively sparse. Gorczyca *et al* studied the optical phonon modes and pressure dependences of AlN and GaN by means of a self-consistent full-potential linear muffin-tin orbital calculation [13]. Kim *et al* investigated the instability of the high-pressure CsCl structure in III–V semiconductors by the DFT linear response method [14]. Goni *et al* studied the effect of pressure on optical phonon modes of GaN and AlN by means of a DFT calculation [11]. Cardona presented a general analysis on the pressure dependence of phonon frequencies for tetrahedrally bonded semiconductors [15]. Thus, a systematic theoretical study on the pressure dependence of the phonon dispersion of III–V semiconductors is essential to provide a comprehensive understanding of the problem.

We have recently thoroughly studied the mechanical and elastic properties of group III–V and IV semiconductors by means of first-principles calculations [16–20]. In this work, we study the pressure effect on phonon and relevant properties for nine common III–V semiconductors by means of linear response DFPT computations. The origins of the unique dielectric and phonon properties in these compounds are traced from their particularities in chemical bonding.

2. The details of the *ab initio* calculation

Our calculation of the phonon frequencies at the Gamma point and dielectric parameters are carried out using density-functional perturbation theory (DFPT) [21–23] in the plane-wave pseudopotential realization using the ABINIT computer code [24]. To achieve a highly efficient calculation without loss of accuracy, the Hartwigsen–Goedecker–Hutter (HGH) relativistic separable dual-space Gaussian pseudopotentials [25] in the context of the local density approximation (LDA) are employed. The condition of hydrostatic pressure is simulated in the same way as in our previous work [16].

There are three main steps in the procedure of our DFPT calculation. Firstly, a self-consistent ground state computation is performed, taking the total symmetry into consideration

Table 1. The *ab initio* dielectric constants, dynamic effective charges, and phonon frequencies at the Γ point from the DFPT calculation. The data in the lines below the calculated value for each phase are from the available experiments.

	ε_∞	ε_s	Z^*	$\omega_{LO}-\omega_{TO}$ (cm^{-1})	ω_{LO} (cm^{-1})	ω_{TO} (cm^{-1})
AlN	4.508	8.373	2.539	243.54	914.70	671.16
	4.6 [26]	8.5 [26]				
AlP	8.323	10.514	2.213	54.25	492.09	437.83
		9.8 [32]	2.28 [34]			443.31 [39]
AlAs	9.404	11.42	2.141	36.37	393.13	356.75
		10.06 [32]	2.18 [3]	42.6 [36]	404.08 [32]	362.14 [32]
			2.20 [36]		402.9 [36]	360.3 [36]
GaN	4.942	9.574	2.552	205.95	731.51	525.56
	5.3 [27]	9.7 [27]	2.65 [11]	189.0 [11]	743.0 [11]	553.0 [11]
GaP	9.495	10.773	1.836	27.76	453.60	425.84
	9.11 [31]	11.1 [32]	2.04 [35]			
GaAs	12.302	14.08	2.016	18.90	289.55	270.65
	10.89 [31]	12.5 [32], 12.9 [31]	2.07 [3]		285.0 [32]	267.3 [32]
			2.18 [36]			
InN	6.723	11.241	2.694	140.86	621.53	480.67
	5.8 [28], 8.4 [33]	13.1 [29]			694 [30]	478 [30]
					586 [37, 38]	472 [37, 38]
InP	9.706	12.172	2.360	37.25	348.04	310.79
	9.61 [31]	12.4 [32], 12.5 [31]	2.55 [35]		344.5 [8]	303.3 [8]
InAs	13.559	16.04	2.409	19.20	237.94	218.74
	12.3 [31]	14.6 [32], 15.15 [31]	2.53 [35]			

for generating the k points in the irreducible Brillouin zone and using the optimized cell parameters of these phases [16, 17]. Then, a non-self-consistent linear response function computation of the $\mathrm{d}/\mathrm{d}k$ perturbation [22] along the x-direction is performed, counting on the cubic symmetry of the zinc-blende phase. This step reads the wavefunctions in the former step and outputs $\mathrm{d}/\mathrm{d}k$ wavefunctions for the following calculation. Finally, there are self-consistent response function computations for electric field perturbations and the ionic displacements. It is known that the accuracy of the DFPT result is sensitively affected by the energy cut-off and the k point sampling in the calculation. The optimum plane-wave energy cut-off for each phase is carefully tested in order to keep the total energy error at 0.001 Hartree. These values vary from 35 Hartree for GaAs to 80 Hartree for GaN. Three k point samplings, $8 \times 8 \times 8$, $10 \times 10 \times 10$, and $12 \times 12 \times 12$, are used in present study. We found that $8 \times 8 \times 8$ sampling is already good enough for most of these phases in lattice dynamics calculations, except for GaP and InN, where good results can only be guaranteed for $10 \times 10 \times 10$ or higher sampling.

3. Numerical results

3.1. Dynamic and dielectric properties

Our first-principles results of the dynamic and dielectric parameters for the nitrides, phosphides, and arsenides of aluminium, gallium, and indium at their equilibrium states are presented in table 1. Where, the phonon frequencies, LO–TO splitting $\omega_{LO}-\omega_{TO}$, high-frequency dielectric coefficient ε_∞, and dynamic effective charge Z^* are directly obtained from the electric field perturbed DFPT calculations. The static dielectric coefficient ε_s is calculated using the Lyddane–Sachs–Teller relation

$$\frac{\omega_{\mathrm{TO}}^2}{\omega_{\mathrm{LO}}^2} = \frac{\varepsilon_\infty}{\varepsilon_{\mathrm{s}}}. \tag{1}$$

The data in the lines below the calculated value for each phase are from the available experiments, in the table.

It is seen from the table that the consistency of theoretical and experimental results is quite satisfactory in general.

3.2. Pressure dependence of lattice dynamical properties

The pressure dependence of the lattice dynamical properties is an important issue for exploring the physics of transport, optical, and thermodynamic behaviours of semiconductors. The volume dependence of the dynamic effective charge Z^*, or the transverse effective charge or Born effective charge, is closely related to the pressure dependence of the ionicity of the chemical bond and is essential for understanding the structural properties. The pressure dependence of the lattice dynamics parameters for the nine common III–V phases in the zinc-blende structure is studied by changing the volume of the primitive cell in our first-principles calculation.

From the Murnaghan equation of state, the hydrostatic pressure is related to the volume variation by

$$p = \frac{B_0}{B_0'}\left[\left(\frac{V_0}{V}\right)^{B_0'} - 1\right] \tag{2}$$

where B_0 denotes the bulk modulus, B_0' is the pressure derivative of B at $p = 0$, $V_0 = a_0^3/4$ is the volume of the primitive unit cell at the equilibrium lattice constant a_0. The *ab initio* values of these parameters used in present study can be found elsewhere [17]. We change the cell dimension a/a_0 from 1.00 to 0.96 in steps of 0.004 to study the volume dependence of the phonon dispersion. There is a wide pressure range under the same volume variation due to the different hardnesses of these phases. Therefore, the theoretical Z^*–$\Delta a/a_0$, ε–$\Delta a/a_0$, and $\Delta\omega$–$\Delta a/a_0$ relationships are given instead in the present results for a better comparison among these phases. It is easy to obtain the corresponding pressure relationships through equation (2).

Our theoretical Z^*–$\Delta a/a_0$ curves are presented in figure 1. It is seen that a perfect linear relationship exists between Z^* and $\Delta a/a_0$ for all these phases. Another significant feature can be noted: that Z^* always decreases with pressure. These relationships can be divided into two groups: Z^* for GaP, GaAs, InP, and InAs changes much rapidly than those for the rest of the phases, marked as $\mathrm{d}Z^*/\mathrm{d}k > 4.0$ ($k = \Delta a/a_0$) or $\mathrm{d}Z^*/\mathrm{d}p < -10^{-2}$ GPa^{-1}. This phenomenon is explained by the analysis of charge transference in section 4. The theoretical ε_∞–$\Delta a/a_0$ curves are presented in figure 2. Figures 1 and 2 show that the pressure dependences of both the dynamic effective charge and the dielectric constant are sensitively related to the type of anion in the compound. Arsenides have the strongest dependence, nitrides the weakest. Our *ab initio* results for the pressure dependences of LO–TO splitting are presented in figure 3. The phases with positive pressure coefficients of the LO–TO splitting are found to be AlN, GaN, and InN, while the others have negative ones. The pressure dependences of these parameters are quantitatively summarized in table 2, where the mode Grüneisen parameters of LO and TO waves at the Γ point, defined by

$$\gamma_{\mathrm{i}} = -\frac{\partial \ln \omega_{\mathrm{i}}}{\partial \ln V} = \frac{B_0}{\omega_{\mathrm{i}}}\frac{\mathrm{d}\omega_{\mathrm{i}}}{\mathrm{d}p}, \tag{3}$$

are also presented. The data in the lines below the calculated value for each phase are from the available previous publications, in the table.

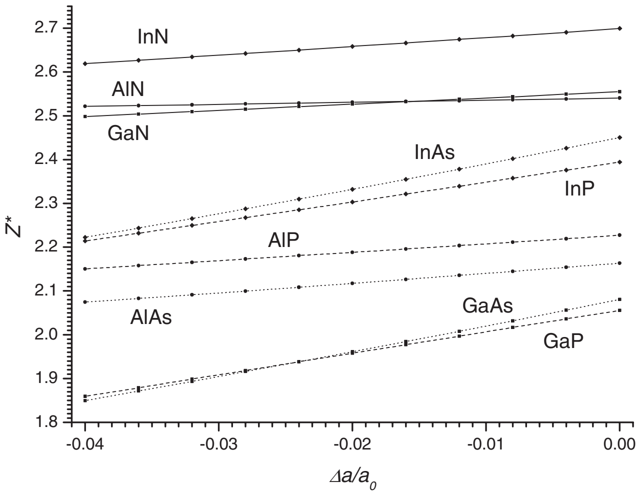

Figure 1. The *ab initio* Z^*–$\Delta a/a_0$ relationships for the nine III–V compounds.

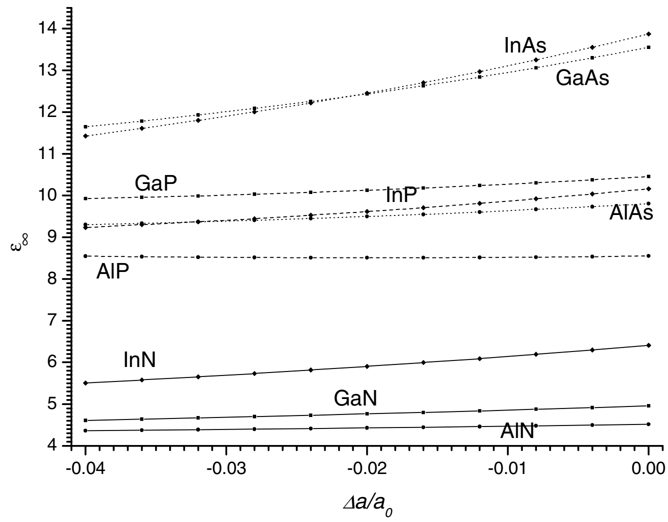

Figure 2. The *ab initio* ε_∞–$\Delta a/a_0$ relationships for the nine III–V compounds.

3.3. Pressure dependence of localized, non-localized charges and polarity

There are three well-established empirical models for studying the lattice dynamics of zinc-blende crystals, i.e. the valence force field model (VFF) [46, 47], the bond–orbital model (BOM) [48, 49], and the bond charge model (BCM) [50, 51]. In the VFF model, Lucovsky *et al* divide the dynamic effective charge Z^* into localized and non-localized parts [35]:

$$Z^* = Z_l^* + Z_{nl}^*. \tag{4}$$

The localized dynamic charge Z_l^* is responsible for dipole–dipole interactions which are closely related to the TO phonon frequency. Z_{nl}^* is the non-localized charge which is distributed

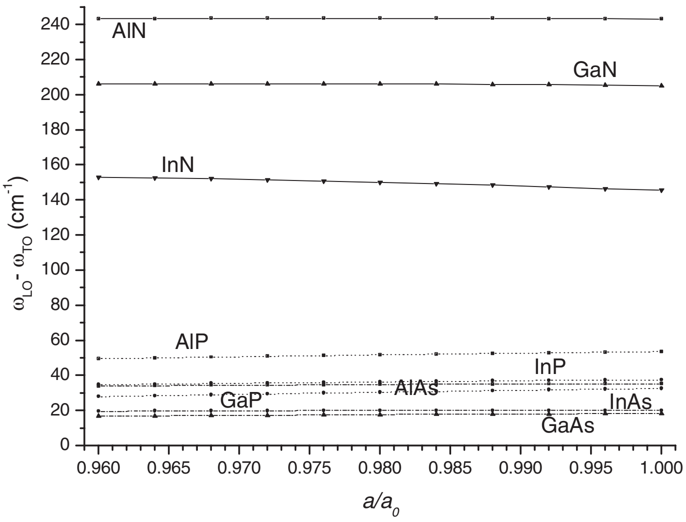

Figure 3. The variations of LO–TO splits with pressure for the nine III–V compounds.

throughout the unit cell. The Z_1^* data for these compounds are calculated following the procedure in [35] using (in cgs units)

$$Z_1^* = \frac{\frac{1}{2}\left(\frac{16}{3}\right)^2\left(\frac{e^2}{\mu\Omega}\right)(C_{11}^* + C_{12}^*) - \omega_{TO}^2}{0.0087\left(\frac{16}{3}\right)^2\left(\frac{e^2}{\mu\Omega}\right) + \frac{4\pi e^2}{3\mu\Omega}} \tag{5}$$

where μ is the reduced mass of the pair of ions, Ω is the volume per pair. Our study shows that Z_1^* always increases with pressure.

In Harrison's BOM, the dynamic charge is related to the polarity α_P of the compound by [48, 52]

$$Z^* = -\Delta Z + 4\alpha_p + 4\alpha_P(1 - \alpha_P^2) \tag{6}$$

where $\Delta Z = 1$ for III–V compounds. The Phillips ionicity f_i is calculated from α_P using

$$f_i = 1 - (1 - \alpha_p^2)^{3/2}. \tag{7}$$

Garcia and Cohen defined a charge asymmetry coefficient g for scaling the polarity in solids [53]. The g parameter measures the strength of the symmetric and anti-symmetric components of the static charge density over the whole unit cell of the phase. g can be directly calculated in the present study. The numerical results for these parameters are listed in table 3. The calculated pressure dependences of the polarity α_P for these compounds are drawn in figure 4. Table 3 shows that the consistency of the present results and the available previously published ones is quite satisfactory. Just as observed by Garcia and Cohen [53], there is a larger deviation between g and f_i parameters especially for nitride phases. This may be understood since f_i included both dynamic and static effects of the charge distribution, while there is only a static effect considered in g. For covalent compounds of strong ionicity with large α_P, the dynamic effect becomes more important.

According to Weber's BCM, the valence charge or bond charge between two bonding ions is such that they can be treated as independent lattice particles with zero mass. These bond charges are allowed to move adiabatically [50, 51]. We calculated the *ab initio* charge densities $q(r)$ along the bond in these compounds. r is the distance to the cation along the

Table 2. Pressure dependences of the phonon dispersions of semiconductors ($k = \Delta a/a_0$). The data in the lines below the calculated value for each phase are from the available previous publications.

	$d\varepsilon_\infty/dk$	$d\varepsilon_\infty/dp$ (10^{-3} GPa^{-1})	dZ^*/dk	dZ^*/dp (10^{-3} GPa^{-1})	$d\omega_{LO}/dp$ (cm^{-1} GPa^{-1})	$d\omega_{TO}/dp$ (cm^{-1} GPa^{-1})	$d(\omega_{LO}-\omega_{TO})/dk$ (cm^{-1})	$d(\omega_{LO}-\omega_{TO})/dp$ (cm^{-1} GPa^{-1})	γ_{LO}	γ_{TO}
AlN	4.37	−4.74	0.47	−0.58	4.17	4.15	−16.74	0.025	0.93	1.26
				−0.90 [43]					1.0 [9]	1.6 [9]
AlP	3.21	−9.73	1.92	−5.45	5.15	5.44	91.97	−0.290	0.94	1.12
										1.36 [39]
AlAs	16.71	−41.60	2.23	−7.44	4.88	5.00	25.76	−0.115	0.96	1.07
			5.8 [36]						1.048 [45]	1.176 [45]
									0.94 [36]	1.14 [36]
GaN	9.81	−10.57	1.41	−1.71	3.74	3.66	−54.78	0.081	1.08	1.47
				−1.8 [40]					1.20 [11]	1.40 [11]
				−1.8 [43]					1.02 [43]	1.19 [43]
GaP	18.15	−55.94	4.91	−13.17	4.10	4.41	109.34	−0.322	0.95	1.10
									0.95 [8]	1.09 [8]
									0.96 [41]	1.19 [41]
									0.87 [44]	1.07 [44]
									1.086 [45]	1.119 [45]
GaAs	57.64	−210.78	5.77	−18.60	3.50	3.82	32.14	−0.134	0.99	1.09
			4.4 [8]						1.09 [44]	1.29 [44]
			4.8 [36]						1.23 [9]	1.39 [9]
									1.24 [41]	1.46 [41]
									1.115 [45]	1.206 [45]
InN	25.71	−49.36	2.01	−3.43	4.92	4.60	−226.29	0.321	1.27	1.52
InP	28.34	−106.57	4.50	−14.94	4.71	4.95	57.57	−0.242	1.02	1.19
			4.5 [8]				65 [8]		1.24 [9]	1.44 [9]
									1.04 [41]	1.34 [41]
									1.19 [44]	1.48 [44]
									1.167 [45]	1.326 [45]
InAs	72.97	−327.61	5.69	−22.42	4.07	4.06	19.28	−0.070	1.06	1.16
									1.06 [42]	1.21 [42]
									1.14 [41]	1.43 [41]

Table 3. The localized and non-localized effective charges, polarities and their pressure dependence ($k = \Delta a/a_0$). The data in the lines below the calculated value for each phase are from the available previous publications.

	Z_l^*	dZ_l^*/dp (10^{-3} GPa^{-1})	dZ_l^*/dk	Z_{nl}^*	α_P	$d\alpha_P/dp$ (10^{-3} GPa^{-1})	$d\alpha_P/dk$	f_i	g
AlN	1.594	8.05	−7.170	0.945	0.508	−0.14	0.095	0.361	0.890
								0.360 [56]	0.794 [53]
								0.449 [57]	
AlP	1.432	32.70	−9.294	0.781	0.449	−1.18	0.339	0.287	0.430
					0.47 [54]			0.307 [57]	0.425 [53]
AlAs	1.318	43.54	−12.618	0.823	0.437	−1.63	0.386	0.272	0.348
					0.44 [54]			0.274 [57]	0.375 [53]
GaN	1.978	9.35	−7.907	0.574	0.511	−0.41	0.286	0.365	0.892
								0.360 [56]	
								0.500 [57]	0.780 [53]
GaP	1.442	36.21	−11.116	0.394	0.419	−2.57	0.811	0.251	0.394
	1.41 [35]				0.48 [55]			0.270 [58]	0.371 [53]
								0.327 [57]	
GaAs	1.253	54.97	−13.286	0.763	0.423	−3.79	0.954	0.256	0.404
	1.28 [35]				0.47 [55]			0.260 [58]	0.316 [53]
								0.310 [57]	
InN	1.972	19.05	−9.643	0.722	0.542	−0.93	0.438	0.406	0.947
								0.578 [57]	0.853 [53]
								0.360 [56]	
InP	1.523	51.45	−11.970	0.837	0.479	−3.45	0.828	0.324	0.561
	1.61 [35]				0.55 [55]			0.370 [56]	0.506 [53]
								0.421 [57]	
InAs	1.323	69.07	−14.211	1.086	0.490	−5.46	1.061	0.338	0.478
	1.16 [35]				0.51 [55]			0.357 [57]	0.450 [53]

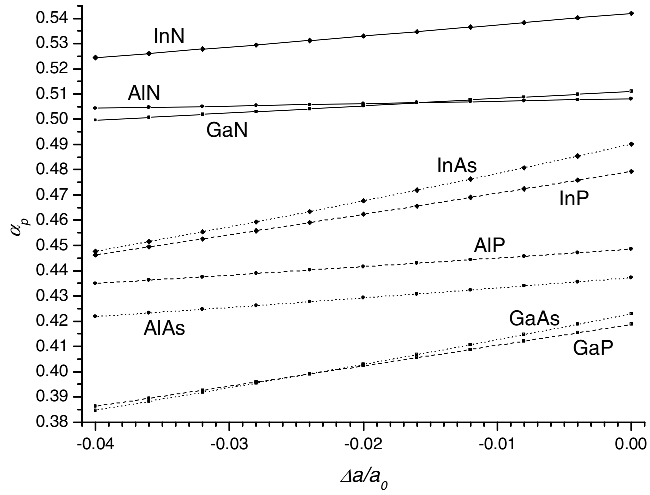

Figure 4. The *ab initio* polarity α_P–$\Delta a/a_0$ relationships for the nine III–V compounds.

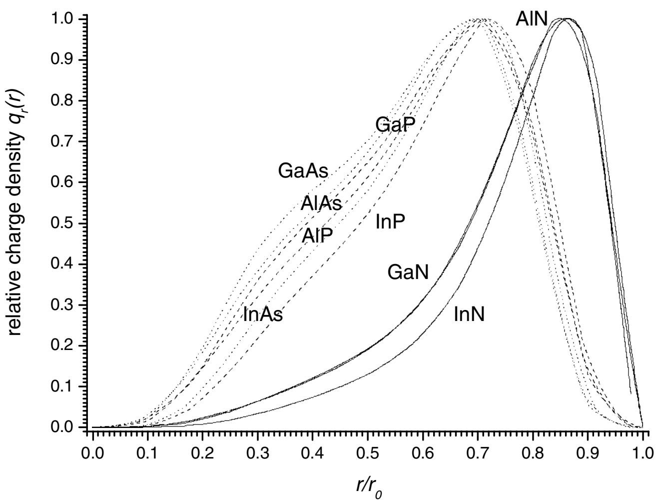

Figure 5. The relative charge density distributions from cation to anion along the bond direction for nine III–V compounds. r_0 is the equilibrium distance from cation to anion. The solid, dashed, and dotted lines are for nitrides, phosphides, and arsenides, respectively.

bond. The relative bond charge density distributions $q_r(r) = q(r)/q(r_m)$ from cation to anion along the bond for the nine III–V compounds are presented in figure 5, where the maximum charge density is at r_m, r_0 is the equilibrium distance between the cation and anion. The solid, dashed, and dotted lines are respectively for nitrides, phosphides, and arsenides in the figure. It is seen that the maximum charge densities are at $r/r_0 \approx 0.7$ for all the phosphide and arsenide compounds, which is in accordance with previous report by Chelikowsky and Cohen [59]. However, the maximum positions for nitrides are significantly different, at $r/r_0 \approx 0.85$. This indicates that the ionicity of III nitride compounds is much stronger than those for the others. In addition to the charge density maximum location, the position of the weighted bond charge

Table 4. Analysis of the first-principles valence charge densities and their pressure dependences ($k = \Delta a/a_0$).

	r_m/r_0	dr_m/dp (10^{-3} nm GPa^{-1})	dr_m/dk (nm)	r_w/r_0	dr_w/dp (10^{-3} nm GPa^{-1})	dr_w/dk (nm)	$\Delta\chi$
AlN	0.860	−0.31	0.206	0.743	−0.24	0.167	1.43
AlP	0.711	−0.50	0.167	0.591	−0.56	0.174	0.58
AlAs	0.698	−1.39	0.337	0.567	−0.70	0.175	0.57
GaN	0.848	−0.23	0.189	0.744	−0.20	0.165	1.23
GaP	0.700	−0.43	0.161	0.585	−0.43	0.162	0.38
GaAs	0.700	−1.16	0.359	0.560	−0.53	0.163	0.37
InN	0.865	−0.36	0.211	0.772	−0.32	0.187	1.26
InP	0.712	−0.61	0.183	0.622	−0.61	0.185	0.41
InAs	0.706	−1.27	0.323	0.598	−0.73	0.186	0.40

density centre, defined by

$$r_w = \frac{\sum_i r_i q(r_i)}{\sum_i r_i}, \tag{8}$$

is also useful for determining the actual bond charge position. The closer to 0.5 r_w/r_0 is, the greater the charge of the bond. Our numerical results on the maximum and weighted bond charge positions r_{max} and r_w, and their pressure dependences, are listed table 4. The last column of table 4 gives the difference in Pauling electronegativity calculated using $\Delta\chi = |\chi(A) - \chi(B)|$, for a binary AB compound.

4. Discussion

The dynamic effective charge is a parameter used to describe the charge behaviour under thermodynamic lattice vibration in crystal. The lattice vibration and the dynamic effective charge originate from the thermodynamic movement of atoms in the crystal. The VFF model, BOM, and BCM are developed to investigate the dynamic behaviour of the lattice. Just like in traditional considerations, the VFF model and the BOM put all the positive and negative charges at cation and anion sites respectively. In contrast, the BCM assumes that the charges at the sites of nominal cations and anions are both positive. The negative charge is accumulated around the bond between the two ions. All the theoretical works so far have shown that the BCM is a much better empirical model as regards reproducing the experimental observations for lattice dynamics than the others. This we attempt to explain as follows.

We give the calculated pressure dependences of Z^* and Z_l^* respectively in tables 2 and 3. The relations of the two dependences are drawn in figure 6. It is seen from the figure that there is a perfect linear relationship between dZ^*/dp and dZ_l^*/dp for the compounds of the same group III element. Z^* decreases with pressure, which linearly corresponds with the increase of Z_l^*. Z_{nl}^*, of course, also decreases with pressure, following equation (4). Similar linear relationships exist among dZ_l^*/dp, dr_w/dp, and dZ^*/dp as shown in figures 7(a) and (b). The decrease of r_w indicates that more bond charge moves toward the middle of the bond. This results in an increase of Z_l^* and decreases of Z_{nl}^* and Z^*, and also a decrease of the polarity. A clear picture of the lattice dynamics can be drawn from the above information on the pressure dependence: the localized dynamic effective charge Z_l^* in the VFF model corresponds to the bond charge in the BCM which is localized around the bond. Z_{nl}^* is from the non-bond charge which is distributed around the ions. The contribution to the dynamic effective charge is from the dynamic behaviours of both bond and non-bond charges. The

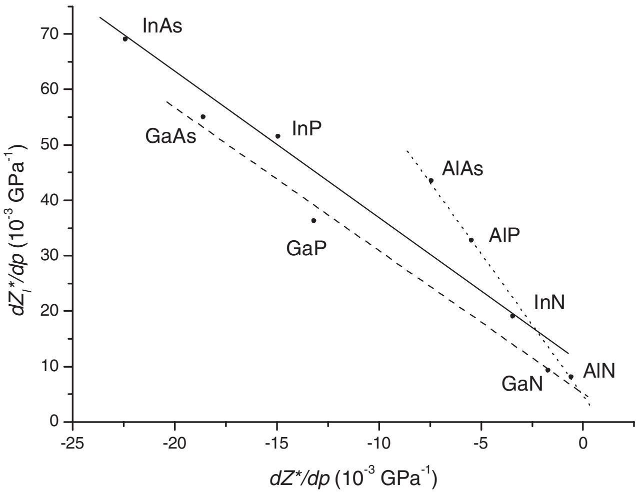

Figure 6. The dZ^*/dp and dZ_l^*/dp relationships for the nine III–V compounds.

more non-localized non-bond charges transform to localized bond charges under the higher pressure. The effect enhances the chemical bonding but weakens the polarity or ionicity of the compound. The most obvious examples of the effect can be seen in GaP, GaAs, InP, and InAs. Table 4 shows that the Pauling electronegativities $\Delta\chi$ of these compounds are all quite small. The charge attractions from the anions are quite weak. Therefore there is the most charge transformation from non-localized to localized regions, which causes the largest dynamic effective charge variation under pressure. The phonon dispersion and dielectric behaviour of III–V semiconductors under pressure are the direct results of this charge transference.

From the results in figures 1–5 it is seen that the group III nitrides exhibit quite different features, as regards lattice dynamics, to the other III–V compounds. The reason for these differences may be explored on the basis of the unique bonding character of group III nitrides. It is known from table 4 that the Pauling electronegativities of nitride phases are several times larger than those of other III–V semiconductors, which results in a much stronger ionicity in the inter-atomic bond of nitrides as compared with those for the other III–V phases. The attraction between the valence electron and anion in a nitride crystal is so strong that valence electrons are tightly bound around the anions. Therefore, the charge distribution is less affected by hydrostatic pressure. The situation is confirmed by the quite small dr_m/dp and dr_w/dp values seen for nitrides in table 4. This is further verified by the much smaller dZ_l^*/dp for nitrides in table 3. The quite large LO–TO splitting in nitrides is a reflection of the strong ionicity in their covalent bonds. Positive pressure coefficients of the LO–TO splitting are found for all nitride phases, which is in accordance with the theoretical results obtained by Goni *et al* [11].

5. Conclusions

First-principles calculations in density-functional perturbation theory are carried out to study the pressure dependences of phonon and dielectric properties for nine common III–V semiconductors. Our results show that the dielectric constant, dynamic effective charge, and polarity decrease, while the localized effective charge and optical phonon frequencies increase with pressure for all these III–V phases. These unique behaviours are reasonably well explained by local charge transference to the bonding region under pressure and hence strengthening of

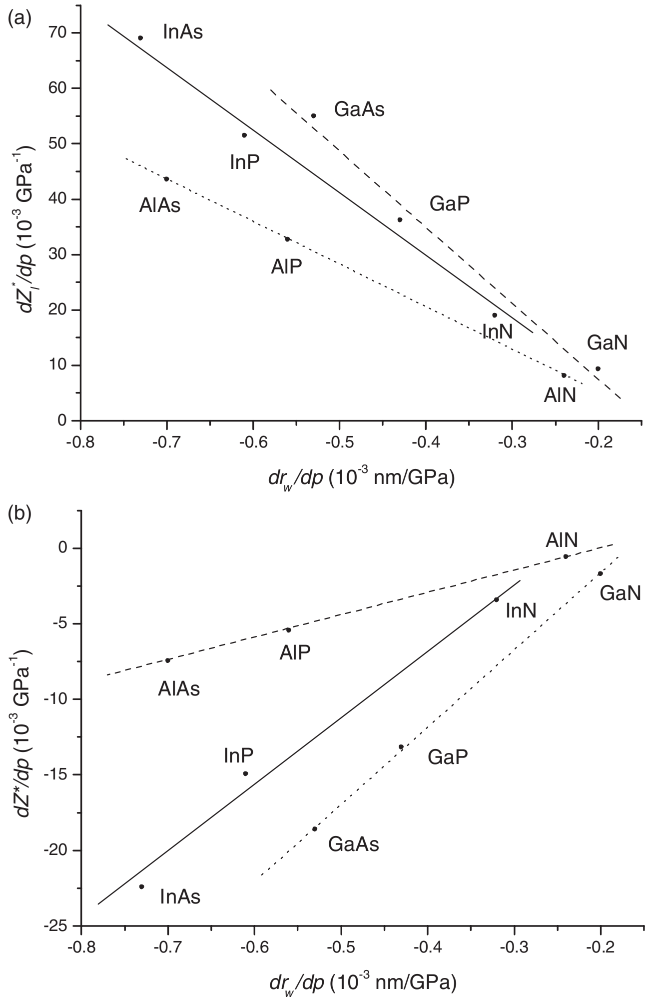

Figure 7. The relationships of pressure derivatives among Z^*, Z_l^* and r_w for the nine III–V compounds. (a) $\mathrm{d}Z_l^*/\mathrm{d}p$–$\mathrm{d}r_w/\mathrm{d}p$, (b) $\mathrm{d}Z^*/\mathrm{d}p$–$\mathrm{d}r_w/\mathrm{d}p$.

the covalent combination of the compound. The difference in pressure dependence of the dynamic behaviour between nitrides and other III–V phases are explained on the basis of the strong ionicity character of the inter-atomic bonds of nitrides.

Acknowledgments

The authors would like to acknowledge the financial support of this work by the National Natural Science Foundation of China (No 50472085) and the Special Funds for the Major State Basic Research Projects of China (No G2000067104).

References

[1] Baroni S, de Gironcoli S and Dal Corso A 2001 *Rev. Mod. Phys.* **73** 515
[2] Kunc K and Martin M 1981 *Phys. Rev.* B **24** 2311

[3] Giannozzi P, de Gironcoli S, Pavone P and Baroni S 1991 *Phys. Rev.* B **43** 7231
[4] Wei S and Chou M Y 1992 *Phys. Rev. Lett.* **69** 2799
[5] Baroni S, de Gironcoli S and Giannozzi P 1990 *Phys. Rev. Lett.* **65** 84
[6] Edwards A L and Drickamer H G 1961 *Phys. Rev.* **122** 1149
[7] Weinstein B A and Piermarini G J 1975 *Phys. Rev.* B **12** 1172
[8] Trommer R, Muller H and Cardona M 1980 *Phys. Rev.* B **21** 4869
[9] Sanjurjo J A, Lopez-Cruz E, Vogl P and Cardona M 1983 *Phys. Rev.* B **28** 4579
[10] Klotz S, Besson J M, Braden M, Karch K, Pavone P, Strauch D and Marshall W G 1997 *Phys. Rev. Lett.* **79** 1313
[11] Goni A R, Siegle H, Syassen K, Thomsen C and Wagner J M 2001 *Phys. Rev.* B **64** 35205
[12] Perlin P, Suski T, Ager J W, Conti G, Polian A, Christensen N E, Gorczyca I, Grzegory I, Weber E R and Haller E E 1999 *Phys. Rev.* B **60** 1480
[13] Gorczyca I, Christensen N E, Blanca E L P and Rodriguez C O 1995 *Phys. Rev.* B **51** 11936
[14] Kim K, Ozolins V and Zunger A 1999 *Phys. Rev.* B **60** R8449
[15] Cardona M 2004 *Phys. Status Solidi* **241** 3128
[16] Wang S Q and Ye H Q 2002 *J. Phys.: Condens. Matter* **14** 9579
[17] Wang S Q and Ye H Q 2002 *Phys. Rev.* B **66** 235111
[18] Wang S Q and Ye H Q 2003 *J. Phys.: Condens. Matter* **15** 5307
[19] Wang S Q and Ye H Q 2003 *Phys. Status Solidi* b **240** 45
[20] Wang S Q and Ye H Q 2003 *J. Phys.: Condens. Matter* **15** L197
[21] Baroni S, Gianozzi P and Testa A 1987 *Phys. Rev. Lett.* **58** 1861
[22] Gonze X 1997 *Phys. Rev.* B **55** 10337
[23] Gonze X and Lee C 1997 *Phys. Rev.* B **55** 10355
[24] Gonze X, Beuken J M, Caracas R, Detraux F, Fuchs M, Rignanese G M, Sindic L, Verstraete M, Zerah G, Jollet F, Torrent M, Roy A, Mikami M, Ghosez P, Raty J Y and Allan D C 2002 *Comput. Mater. Sci.* **25** 478
[25] Hartwigsen C, Goedecker S and Hutter J 1998 *Phys. Rev.* B **58** 3641
[26] Goldberg Yu 2001 *Properties of Advanced Semiconductor Materials GaN, AlN, InN, BN, SiC, SiGe* ed M E Levinshtein, S L Rumyantsev and M S Shur (New York: Wiley) pp 31–47
[27] Bougrov V, Levinshtein M E, Rumyantsev S L and Zubrilov A 2001 *Properties of Advanced Semiconductor Materials GaN, AlN, InN, BN, SiC, SiGe* ed M E Levinshtein, S L Rumyantsev and M S Shur (New York: Wiley) pp 1–30
[28] Inushima T, Shiraishi T and Davidov V Yu 1999 *Solid State Commun.* **110** 491
[29] Davydov V Y, Emtsev V V, Goncharuk A N, Smirnov A N, Petrikov V D, Mamutin V V, Vekshin V A, Ivanov S V, Smirnov M B and Inushima T 1999 *Appl. Phys. Lett.* **75** 3297
[30] Osamura K, Naka S and Murakami Y 1975 *J. Appl. Phys.* **46** 3432
[31] Levinstein M, Rumyantsev S and Shur M 1999 *Handbook Series on Semiconductor Parameters* vol 1, 2 (London: World Scientific)
[32] Palmer D W 2003 http://www.semiconductors.co.uk
[33] Tansley T L 1994 *Properties of Group III Nitrides* ed J H Edgar (London: INSPEC)
[34] Christensen N E, Satpathy S and Pawlowska Z 1987 *Phys. Rev.* B **36** 1032
[35] Lucovsky G, Martin R M and Burstein E 1971 *Phys. Rev.* B **4** 1367
[36] Spencer G S, Ho A C, Menendez J, Droopad R, Fathollahnejad H and Maracas G N 1994 *Phys. Rev.* B **50** 14125
[37] Qian Z G, Shen W Z, Ogawa H and Guo Q X 2004 *J. Phys.: Condens. Matter* **16** R381
[38] Kaczmarczyk G, Kaschner A, Reich S, Hoffmann A, Thomsen C, As D J, Lima A P, Schikora D, Lischka K, Averbeck R and Riechert H 2000 *Appl. Phys. Lett.* **76** 2122
[39] Rodriguez C O, Casali R A, Peltzer E L, Cappannini O M and Methfessel M 1989 *Phys. Rev.* B **40** 3975
[40] Sengstag T, Binggeli N and Baldereschi A 1995 *Phys. Rev.* B **52** R8613
[41] Talwar D N and Vandevyver M 1990 *Phys. Rev.* B **41** 12129
[42] Trommer R, Anastassakis E and Cardona M 1976 *Light Scattering in Solids* ed M Balkanski, R C C Leite and S P S Porto (Paris: Flammarion)
[43] Wagner J M and Bechstedt F 2000 *Phys. Rev.* B **62** 4526
[44] Anastassakis E and Cardona M 1998 *High Pressure in Semiconductors Physics* vol 55, ed T Suski and W Paul (New York: Academic)
[45] Debernardi A, Ulrich C, Cardona M and Syassen K 2001 *Phys. Status Solidi* b **223** 213
[46] Martin R M 1970 *Phys. Rev.* B **1** 4005
[47] Keating P N 1966 *Phys. Rev.* **145** 637
[48] Harrison W A 1973 *Phys. Rev.* B **8** 4487

[49] Harrison W A and Ciraci S 1974 *Phys. Rev.* B **10** 1516
[50] Weber W 1974 *Phys. Rev. Lett.* **33** 371
[51] Weber W 1977 *Phys. Rev.* B **15** 4789
[52] Vogl P 1978 *J. Phys. C: Solid State Phys.* **11** 251
[53] Garcia A and Cohen M L 1993 *Phys. Rev.* B **47** 4215
[54] Harrison W A 1980 *Electronic Structure and the Properties of Solids* (San Francisco, CA: Freeman)
[55] Harrison W A 1974 *Phys. Rev.* B **10** 767
[56] Coulson C A, Redei L B and Stocker D 1962 *Proc. R. Soc.* **270** 352
[57] Phillips J C 1970 *Rev. Mod. Phys.* **42** 317
[58] Pauling L 1960 *The Nature of the Chemical Bond* (Ithaca, NY: Cornell University Press)
[59] Chelikowsky J R and Cohen M L 1976 *Phys. Rev.* B **14** 556